



## Article

### *In Situ* FTIR Observation of the Polymer FM Enrichment at the EHL Contact

Reina Goto<sup>1)</sup>, Ko Onodera<sup>1)\*</sup>, Takehisa Sato<sup>1)</sup>, Yasushi Hoshi<sup>2)</sup>, Hidetaka Nanao<sup>2)</sup> and Shigeyuki Mori<sup>2)</sup>

<sup>1)</sup>EMG Lubricants Godo Kaisha, 6-1 Ukishima-cho, Kawasaki-ku, Kawasaki, Kanagawa 210-9526, Japan

<sup>2)</sup>Iwate University, 4-3-5 Ueda, Morioka, Iwate 020-8551, Japan

\*Corresponding author: Ko Onodera (ko.onodera@emglube.com)

Manuscript received 10 November 2019; accepted 03 May 2020; published 15 June 2020

Presented at the International Tribology Conference Sendai 2019, 17-21 September, 2019

#### Abstract

Research interests recently increased in studying polymer-type friction modifiers (polymer FM) consisting of a polymer backbone and a functional group because of their good friction reduction capability. However, there is no clear verification of their working mechanisms. Therefore, the polymer FM behavior at the contact region must be understood to provide mechanistic information and design further-improved polymer FMs. For this purpose, *in situ* observation techniques have been applied to the chemical analysis of the oil film formed from a polymer FM using a micro-Fourier transform infrared spectrometer. The experimental results indicate that the polymer concentrations at the Hertzian contact drastically increased, exceeding the bulk concentration of oil. The following new friction reduction mechanism is proposed based on the clarified polymer FM concentration: the concentrated adsorption layer of the polymer FM prevents direct contact of the surface asperities.

#### Keywords

*in situ* observation, micro-FTIR, polymer, friction modifiers, EHL contact, lubricant film, film thickness, adsorbed layer

#### 1 Introduction

Automobile electrification is expanding to reduce carbon dioxide emissions. The hybridization of a conventional internal combustion engine significantly improves the fuel economy of a vehicle. However, this change will bring about a lower oil temperature, which will affect the design of additive technology in engine oils [1]. Molybdenum dithiocarbamate (MoDTC), which is widely used as a friction modifier (FM) of lubricants for conventional engines, decomposes at high temperature to form a low-friction MoS<sub>2</sub> film on metal surfaces. However, the effect of MoDTC might not be fully expected in hybrid vehicles because of its low oil temperature; hence, FM, which is effective at low oil temperature, is required for next-generation automobile lubricants. Adsorption-type FMs that do not need high temperatures for their performance have become the focus of research to realize friction reduction at low oil temperatures.

Conventionally, small molecules such as oleic acid and glycerol monooleate as adsorption-type FMs were used. Recently, because of their good friction reduction capability, studies focused on new adsorption-type FMs called polymer-type friction modifiers (polymer FM) that consist of a polymer backbone and functional groups. Their performance regarding friction coefficient, oil film thickness, and wear has been examined [2–4]. According to these studies, polymer

FMs, in general, reduce friction at a low speed by forming a thick adsorption film [3]. A few studies focused on the chemical information of the film, including the polymer FM concentrations. To provide mechanistic information for designing further-improved polymer FMs, one must understand their action mechanisms at the contact region. This study focuses on polymer FM concentrations to clarify its working mechanism. There is a need for an *in situ* observation at the contact region because the polymer FM does not form a reaction film that could be analyzed with an *ex-situ* analysis such as X-ray photoelectron spectroscopy and electron probe microanalysis. The polymer FM could easily be removed after washing by an organic solvent before the analysis.

Several studies reported on the result of *in situ* observation tests to understand the behavior of polymers in the past [5–8]. Guanteng et al. showed that some polymers form boundary lubricating film up to 30 nm-thick in slow-speed or high-temperature, rolling, and concentrated contacts by using optical interferometry [5]. Muraki et al. demonstrated that some polymers increase film thickness because of the adsorption of polymer molecules on the surface and reduce friction by using optical interferometry [6]. However, the interferometry technique does not provide chemical information about the oil film. In contrast, the *in situ* Fourier transform infrared spectrometer (FTIR) observation technique that uses a micro-

FTIR could provide quantitative information on additives in the elastohydrodynamic lubrication (EHL) film under dynamic conditions [9–12]. The change of the additive concentration in the EHL film was clarified in a previous study by Hoshi et al. The behavior of oleic acid was also investigated, revealing that the additive concentration decreased in the EHL film [11]. In the present study, *in situ* observation techniques were applied to the chemical analysis of an oil film formed from the polymer FM containing oil to clarify its action mechanism.

## 2 Experimental methods

### 2.1 Test samples

A polymer FM and oleic acid were used as adsorption-type FMs. Both have a functional group that adsorbs on the surface. The polymer FM was composed of a polymethacrylate (PMA) backbone and a hydroxyl group (Fig. 1). The molecular weight of the polymer FM is about 20,000. Table 1 shows the viscosity of the test samples. The polymer FM was diluted at concentrations of 0.8, 2.0, and 4.0 mass% with a base oil mixture of PAO and Gr.III. Oleic acid diluted at a 2.0 mass% concentration was used to represent the low-molecular-weight adsorption-type FMs. All oil viscosities were adjusted to approximately 200 mm<sup>2</sup>/s to provide a sufficiently high viscosity and form the EHL film at the test condition of the *in situ* FTIR test.

### 2.2 Friction test

The friction performances of the oils were evaluated by a PCS Instruments Mini Traction Machine (MTM). Figure 2 shows a schematic diagram of the MTM. In this apparatus, the sample oil was applied to the surface of a rotating disk, a ball is then loaded and rotated against this flat surface. The motion of both parts can be controlled independently, enabling the measurement of the Stribeck curve from the EHL to the mixed lubrication conditions. Table 2 presents the details of the test conditions. The rolling speed was changed during the friction test to acquire the Stribeck curve. The sliding rolling ratio was set as 50% to evaluate the mixed lubrication–EHL condition. The test temperature was set at 40°C to evaluate the FM performance at low temperature.

### 2.3 Oil film thickness measurement

The central oil film thickness was measured by optical interferometry using a PCS Instruments EHD2. In this apparatus, a ball is loaded and rotated against a flat surface of a rotating disk in the presence of the sample oil. The motion of

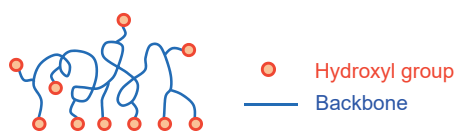


Fig. 1 Structure of the polymer FM

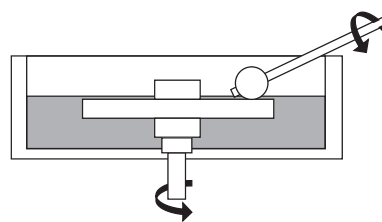


Fig. 2 Schematic diagram of the friction tester

Table 2 Test conditions for the friction test

Test piece material	AISI 52100
Sliding rolling ratio	50%
Load	37 N
Hertzian contact pressure	1.0 GPa
Temperature	40°C
Speed	5–300 mm/s

Table 3 Test conditions for the oil film thickness measurement

Test piece material	Ball	AISI 52100
	Disk	Glass disk with thin Cr and silica layer
Sliding rolling ratio	0%	
Load	10.0 N	
Hertzian contact pressure	0.4 GPa	
Temperature	40°C	
Speed	3–1000 mm/s	

both parts can be controlled independently. Table 3 shows the details of the test conditions. The sliding rolling ratio and the contact pressure were set in a similar range to those in the *in situ* FTIR test described in Section 2.4.

### 2.4 In situ FTIR observation

Micro-FTIR was used in conjunction with a ball-on-disk lubrication tester to analyze the lubricant films under dynamic conditions. Figure 3 depicts a schematic diagram of the *in situ* FTIR tester. The IR spectra were obtained at the positions covering the inlet to the outlet of the Hertzian contact region (Fig. 4). The sampling size was a 50 × 50 μm square, which was smaller than the Hertzian diameters of our test conditions. The IR spectra were obtained at 50 μm intervals along the centerline of the contact.

A CaF<sub>2</sub> disk, which permeated both specific peaks of the base oil and the polymer FM/oleic acid (C–H: 2800–3000 cm<sup>-1</sup>, C=O: 1700–1750 cm<sup>-1</sup>), was used. The polymer FM had multiple carbonyl groups (C=O) in its molecules because it had a PMA backbone, and the oleic acid also contained C=O in its molecule. Table 4 presents the details of the test conditions.

Table 1 Viscosity of the test samples

			Base oil	Base oil + polymer FM			Base oil + oleic acid
Concentration			-	0.8 mass%	2.0 mass%	4.0 mass%	-
Kinematic viscosity	at 30°C*	mm <sup>2</sup> /s	200	196	197	199	198
	at 40°C	mm <sup>2</sup> /s	122	120	121	123	122
	at 100°C	mm <sup>2</sup> /s	16.7	16.2	16.7	17.5	17.0

\*Calculated from KV 40 and KV 100

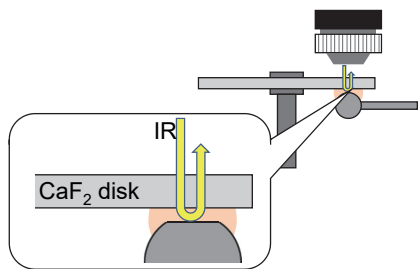


Fig. 3 Schematic diagram of the *in situ* FTIR tester

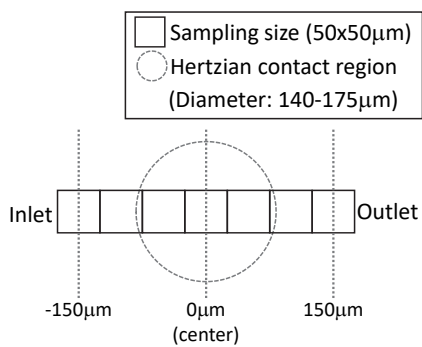


Fig. 4 Sampling positions

Table 4 Test conditions for the *in situ* FTIR test

Test piece material	Ball	AISI 52100
	Disk	CaF <sub>2</sub>
Sliding rolling ratio	0%	
Load	2.5, 4.9 N	
Hertzian contact pressure	0.25, 0.36 GPa	
Temperature	30°C	
Speed	0.26, 0.52 m/s	
Aperture size	50 µm × 50 µm	
Scan number	64	
Scan time	15 s	

Figure 5 shows examples of the IR spectra of the sample oil. Figures 5a and b show an IR spectrum of the C–H stretching mode derived from the base oil and that of the C=O stretching mode derived from the polymer FM or oleic acid, respectively. The polymer FM and oleic acid concentrations were calculated

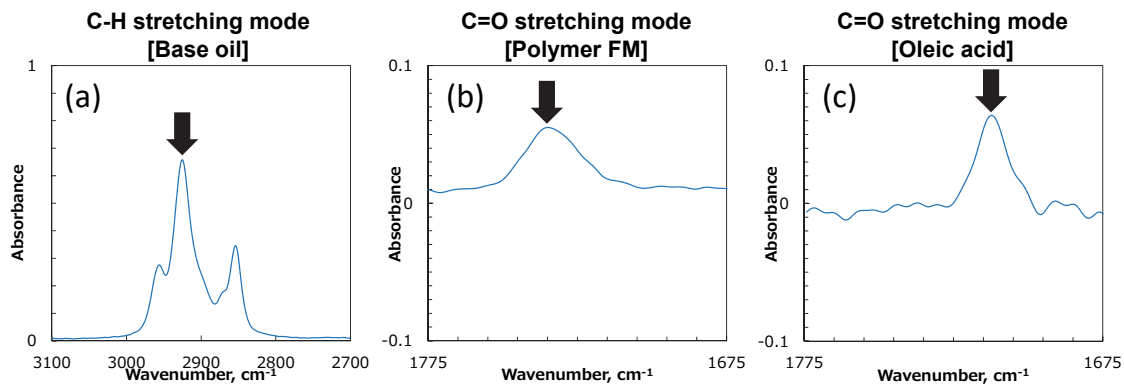


Fig. 5 IR spectra of the sample oil

based on the calibration line of each sample, as exemplified in Fig. 6, where the absorbance ratios of C=O and C–H were plotted against the FM concentration. The plots in the calibration curve were acquired by measuring several different FM concentrations using the same FTIR tester.

### 3 Results

#### 3.1 Friction test

Figure 7 shows the friction performance of the sample oils. The friction coefficient of the base oil was higher at a lower speed in conformity with a typical Stribeck curve. This

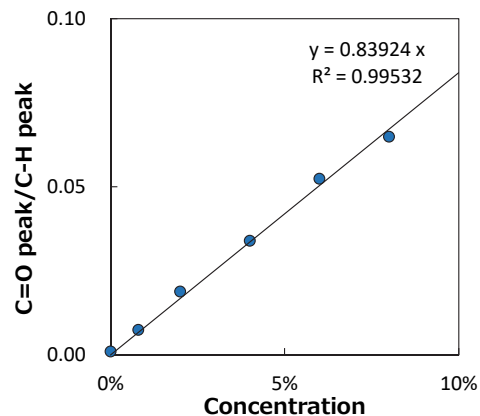


Fig. 6 Calibration curve of the polymer FM solution

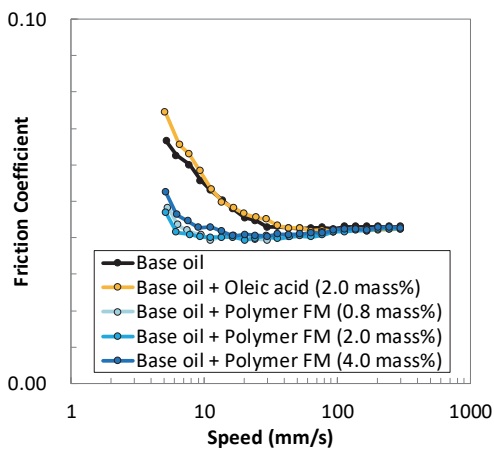


Fig. 7 Comparison of friction performance

curve illustrates mixed lubrication–EHL regime of the typical Stribeck curve, where the regime changes from EHL to mixed lubrication at about 0.1 m/s. Regardless of its concentration under the mixed lubrication regime, the polymer FM showed low friction compared to the base oil alone. In contrast, the friction coefficient of oleic acid was almost the same as that of the base oil, indicating that oleic acid did not reduce the friction under this condition.

3.2 Oil film thickness

Figure 8 shows the results of the oil film thickness measurement. As theoretically expected, the oil film thickness of the base oil became thinner as the rolling speed was lowered. The oil film thickness of the base oil + polymer FM was thicker than that of the base oil alone from low to high-speed ranges, including the rolling speed range of the *in situ* FTIR test. The addition of the polymer FM increased the film thickness to approximately 10 nm, regardless of its concentration from 0.8 to 4.0 mass%. The friction reduction caused by adding the polymer FM observed at the MTM at 0.1 m/s and below could be because of the increase of oil film thickness that prevents metal-metal contact, assuming that a similar increase in oil film thickness occurred [13].

In contrast, the film thickness increased as much as 2 nm by the addition of oleic acid, which well agreed with that previously reported [11]. Considering the rolling speed range, the 250 to 300 nm-thick oil films were expected to form under the conditions in which the *in situ* FTIR test was performed.

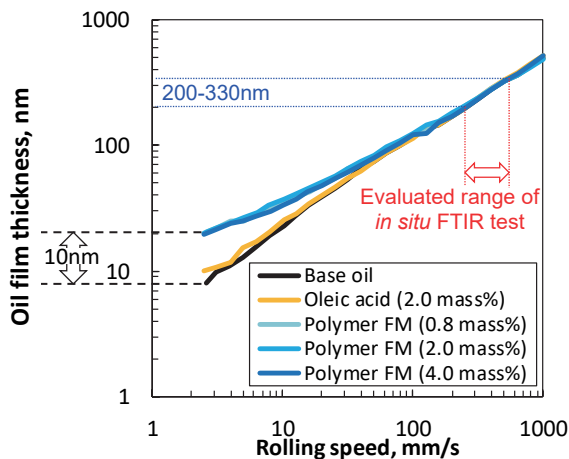


Fig. 8 Comparison of oil film thickness

3.3 In situ FTIR observation result

(1) Polymer FM

(1-1) Effect of the test condition

Figure 9 shows the *in situ* FTIR result of the polymer FM at a 2.0 mass% concentration. Figure 9a shows the absorbance of the C–H stretching mode plotted against the inlet to the outlet positions representing the quantity of the base oil in the oil film, which is an indicator of its thickness. The dotted lines show the calculated Hertzian region at 2.5 N (green) and 4.9 N (blue), respectively. The base oil quantity decreased as it got closer to the center. Regarding the test condition dependence, the base oil quantity was larger under the higher speed, and lower load condition, as theoretically expected.

Figure 9b illustrates the absorbance of the C=O stretching mode representing the polymer FM quantity. The polymer FM quantity was almost the same over the measured positions and test conditions. Figure 9c shows the polymer FM concentration calculated from these two absorbance ratios. The concentration in the EHL film was much higher than the original concentration of 2.0 mass%, especially at the lower speed.

(1-2) Effect of concentration

Figure 10 presents the effect of the polymer FM concentration. In the case of 0.8 mass% and 2.0 mass%, the C–H and C=O stretching modes showed the same trend as in Fig. 9. The concentrations in the Hertzian contact were increased to approximately 2.0 mass% and 4.0 mass%, respectively, which were higher than the bulk concentration of the original oils, as shown in Fig. 10c. In contrast, the result showed a different trend at 4.0 mass% from the two previous oils. The polymer FM concentration decreased at the inlet side to the Hertzian contact.

(2) Oleic acid

Figure 11 shows the oleic acid concentration calculated from the absorbance ratio evaluated through the same method. The oleic acid concentrations in the Hertzian contact region were lower than the original concentration, which agrees with the previous research of Hoshi et al. [11].

3.4 Summary of the evaluations

The confirmed results are as follows:

- i) Friction was reduced by adding the polymer FM under the low-speed condition.
- ii) A 10 nm increase of the oil film thickness by adding the polymer FM was observed from the low to the high-speed range.

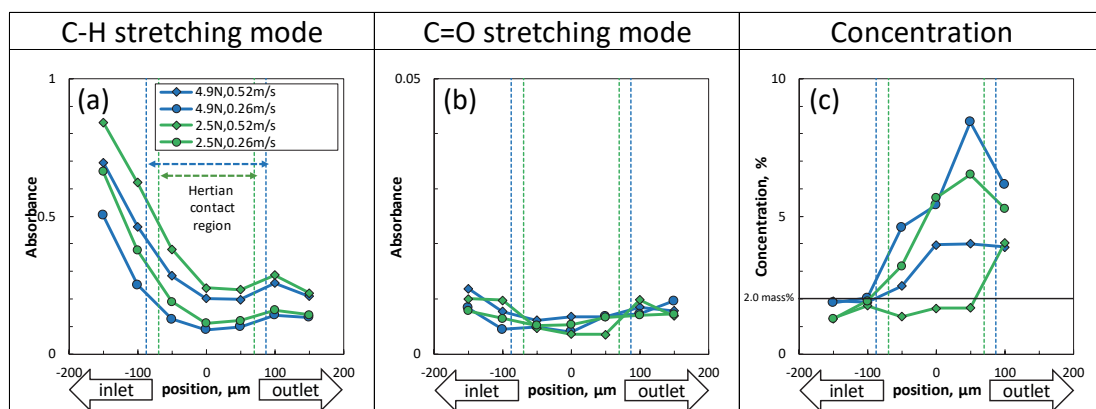


Fig. 9 *In situ* FTIR result of the polymer FM (2.0 mass%)

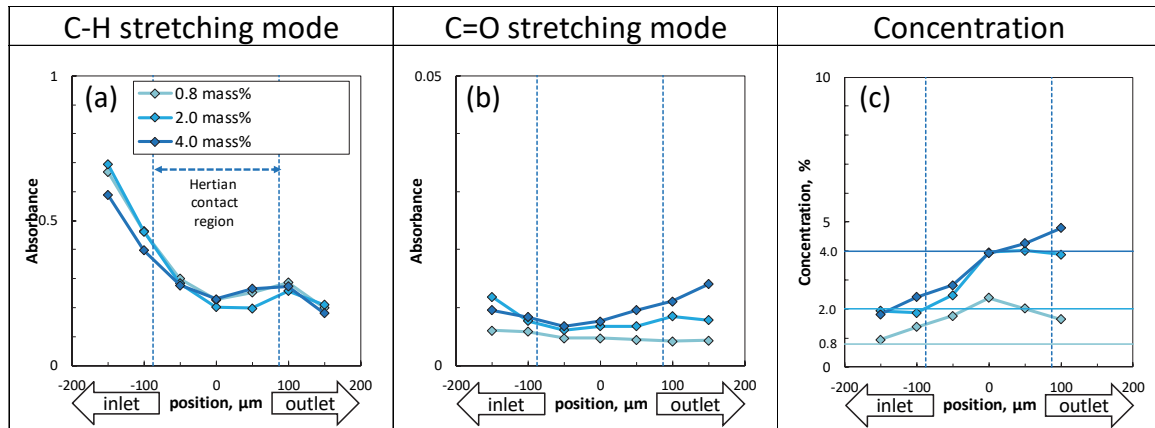


Fig. 10 Effect of the polymer FM concentration

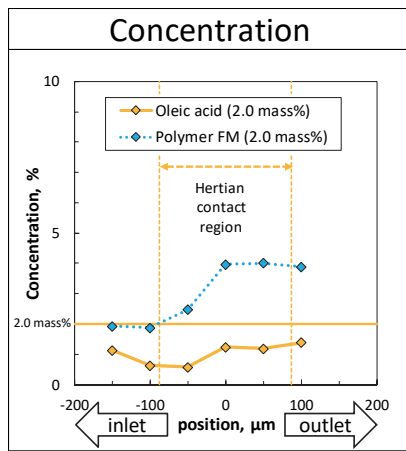


Fig. 11 Concentration of oleic acid in the EHL film

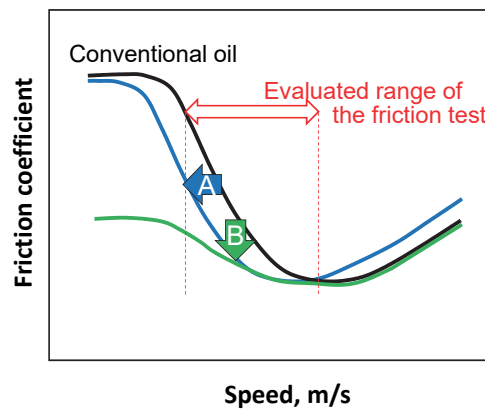


Fig. 12 Assumed Stribeck curve of the low-friction samples

- iii) The polymer FM concentration in the Hertzian contact region was increased.

## 4 Discussion

### 4.1 Assumed low friction mechanisms

The friction of polymer FM was lower than that of the base oil alone under the low-speed condition, which was expected to be the mixed lubrication condition. Two possible mechanisms that bring about the low friction were raised, namely a hydrodynamic effect (mechanism A) and a boundary film effect (mechanism B) (Fig. 12).

Mechanism A assumes that the polymer FM addition would shift the Stribeck curve to the left and widen the hydrodynamic lubrication region; hence, friction will be reduced under the mixed lubrication condition. This would happen if the bulk polymer FM concentration of the inlet in the oil increases in the EHL film to raise the effective viscosity resulting in a thicker oil film formation. Literature supports this mechanism. For example, Guanteng et al. suggested that polymers form viscous surface layers on solid surfaces, which produce enhanced hydrodynamic entrainment under thin-film conditions [5], and Spikes suggested that polymer forms a thin-film of high viscosity on solid surfaces, providing fluid film protection [7]. However, mechanism A could not likely work for the polymer FM because the increase of its concentration at the inlet side was not observed in the *in situ* FTIR measurement.

In contrast, mechanism B assumes that the polymer FM would form an adsorption film on the surface asperities to reduce friction by lowering shear loss and preventing direct contacts between the asperities. The result of the oil film thickness measurement showed a 10 nm-thick film, which was possibly formed by its adsorption. Hence, the polymer FM adsorption could have lowered the friction, as explained by mechanism B.

### 4.2 FM concentration in the EHL film

The polymer FM concentration in the EHL films was analyzed based on the mass balance calculation using the oil and adsorption film thicknesses obtained by the EHL interferometry film measurement and the polymer FM concentration obtained by the *in situ* IR measurement. This analysis was done to quantitatively understand the cause of the low friction based on mechanism B.

The measured oil film thickness at 0.5 m/s speed and 10 N load was 300 nm, which should be the sum of the bulk oil film thickness and the adsorbed film thickness (Fig. 13). The bulk oil film thickness should be 290 nm and obtained by subtracting the adsorbed film thickness of 10 nm. Meanwhile, the polymer FM concentration in the Hertzian contact regions at the same condition was obtained from the *in situ* FTIR measurement.

The polymer FM concentrations are expressed as Eq. (1) using mass balance, where *A* is the concentration in the Hertzian contact, *B* is that in the adsorbed film, and *C* is that in the bulk oil film.



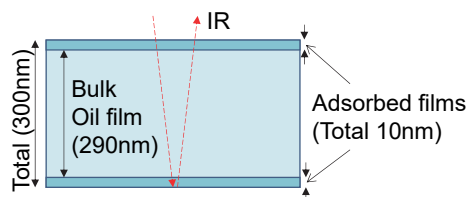


Fig. 13 A schematic model of oil film structure in the EHL film (at 0.5 m/s speed and 10 N load)

$$300A = 10B + 290C \quad (1)$$

In the case of the polymer FM concentration of 2.0 mass%, the average concentration in the Hertzian contact A was 4.0 mass%, as described in Section 3.3. Assuming that the concentration in the bulk oil in the EHL film is the same as the original oil, C becomes 2.0 mass%; thus, the FM concentration of the adsorbed film is 62%. In other words, assuming the formation of the concentrated adsorption film of the polymer FM, the enrichment observed by the *in situ* FTIR was reasonably explained.

The increase of the film was 10 nm; thus, it would be reasonable to assume that 5 nm-thick adsorption films were formed on each surface. A 5 nm thickness is larger than the expected size of the polymer FM. Therefore, we propose the mechanism where the friction coefficient is lowered by the concentrated multiple-layer adsorption film formed by the polymer FM, preventing direct contacts between the surface asperities.

## 5 Conclusions

The low-friction performance of a polymer FM was clarified herein. The mechanism was investigated by EHL interferometry of the oil film and by *in situ* FTIR measurements.

The following conclusions are drawn:

- The polymer FM showed low friction compared to the base oil alone under the mixed lubrication condition.
- A 10 nm increase of the oil film thickness was observed by the polymer FM addition.
- The polymer FM concentration in the Hertzian contact region was higher than the original concentration obtained by the *in situ* FTIR observation in the EHL contact. Based on the mass balance, the polymer FM concentration of the adsorption film was 62%.

Based on the result, this study proposes the following friction reduction mechanism: the concentrated multiple adsorption layer of the polymer FM prevented any direct contact between the surface asperities.

## Acknowledgements

The authors thank Sanyo Chemical Industries, Ltd. for providing the polymer FM samples.

## References

- [1] Onodera, K., Watanabe, H., Sato, T., Lee, G. H., Kaneko, T., Yamamori, K. and Miyata, I., "Fuel Economy Improvement by Engine Oil with Ultra-High Viscosity Index," SAE Technical Paper, 2019-01-2203, 2019.
- [2] Fan, J., Muller, M., Stohr, T. and Spikes, H. A., "Reduction of Friction by Functionalised Viscosity Index Improvers," Tribology Letters, 28, 3, 2007, 287-298.
- [3] Muraki, M., Nakamura, K., Suzuki, M., Segami, T. and Yamamoto, K., "Tribological Properties of Oils Containing Poly-laurylacrylate with Hydroxyethyl Group," Journal of Japanese Society of Tribologists, 59, 8, 2014, 507-514 (in Japanese).
- [4] Moody, G., Eastwood, J. and Ueno, K., "The Performance and Mechanisms of Organic Polymeric Friction Modifiers in Low Viscosity Engine Oils," SAE Technical Paper, 2019-01-2204, 2019.
- [5] Guangteng, G., Smeeth, M., Cann, P. M. and Spikes, H. A., "Measurement and Modelling of Boundary Film Properties of Polymeric Lubricant Additives," Proceedings of the Institution of Mechanical Engineers, Part J: Journal of Engineering Tribology, 210, 1, 1996, 1-15.
- [6] Muraki, M. and Nakamura, K., "Film-Forming Properties and Traction of Non-Functionalized Polyalkylmethacrylate Solutions under Transition from Elastohydrodynamic Lubrication to Thin-Film Lubrication," Proceedings of the Institution of Mechanical Engineers, Part J: Journal of Engineering Tribology, 224, 1, 2010, 55-63.
- [7] Spikes, H. A., "Film-Forming Additives - Direct and Indirect Ways to Reduce Friction," Lubrication Science, 14, 2, 2002, 147-167.
- [8] Cann, P. M. and Spikes, H. A., "The Behavior of Polymer Solutions in Concentrated Contacts: Immobile Surface Layer Formation," Tribology Transactions, 37, 3, 1994, 580-586.
- [9] Cann, P. M. and Spikes, H. A. "In Lubro Studies of Lubricants in EHD Contacts Using FTIR Absorption Spectroscopy," Tribology Transactions, 34, 2, 1991, 248-256.
- [10] Mori, S., "Advanced Analytical Methods in Tribology," Springer, Cham, 2018, 215.
- [11] Hoshi, Y., Shimotomai, N., Sato, M. and Mori, S., "Change of Concentration of Additives under EHL Condition," Journal of Japanese Society of Tribologists, 44, 9, 1999, 736-743 (in Japanese).
- [12] Hoshi, Y., Takiwatari, K., Nanao, H., Yashiro, H. and Mori, S., "In Situ Observation of EHL Films of Greases by Micro Infrared Spectroscopy," Tribology Online, 14, 2, 2019, 53-59.
- [13] Nakamura, K. and Muraki, M., "Traction Behavior of Polyalkylmethacrylate Solutions Accompanied by Transition of Lubrication Regime," Journal of Japanese Society of Tribologists, 53, 9, 2008, 628-635 (in Japanese).



This paper is licensed under the Creative Commons Attribution-NonCommercial-NoDerivatives 4.0 International (CC BY-NC-ND 4.0) International License. This allows users to copy and distribute the paper, only upon conditions that (i) users do not copy or distribute such paper for commercial purposes, (ii) users do not change, modify or edit such paper in any way, (iii) users give appropriate credit (with a link to the formal publication through the relevant DOI (Digital Object Identifier)) and provide a link to this license, and (iv) users acknowledge and agree that users and their use of such paper are not connected with, or sponsored, endorsed, or granted official status by the Licensor (i.e. Japanese Society of Tribologists). To view this license, go to <https://creativecommons.org/licenses/by-nc-nd/4.0/>. Be noted that the third-party materials in this article are not included in the Creative Commons license, if indicated on the material's credit line. The users must obtain the permission of the copyright holder and use the third-party materials in accordance with the rule specified by the copyright holder.